THE ASTROPHYSICAL JOURNAL, 496:376–385, 1998 March 20

HYDROGEN-ACCRETING CARBON-OXYGEN WHITE DWARFS

SANTI CASSISI,[1,2] ICKO IBEN, JR.,[3] AND AMEDEO TORNAMBÈ[2]
Received 1997 September 11; accepted 1997 October 30

ABSTRACT

Matter of solar system composition has been added to the surfaces of two initially cool carbon-oxygen (CO) white dwarfs of masses 0.5 $M_\odot$ and 0.8 $M_\odot$ at rates in the range 10^{-8} to 10^{-6} $M_\odot$ yr^{-1}. Four different regimes are encountered. (1) At the highest accretion rates, models become red giants after the accretion of only a very small amount of mass. As the accretion rate is decreased, models are encountered that (2) burn hydrogen at the same rate at which it is accreted, (3) experience a series of nondynamical hydrogen shell flashes followed eventually by a powerful helium shell flash, and, finally, (4) experience nova-like hydrogen shell flashes.

Although all of the regimes have been explored, special attention has been given to models that experience recurrent mild hydrogen-burning pulses or burn hydrogen at a stationary rate. For lower accretion rates, the helium flash is so powerful that the convective layer forced by helium burning penetrates deeply into the hydrogen-rich envelope; this penetration may lead to the ejection of external layers even if the helium flash would not of itself have become dynamical. For higher accretion rates, even when convection does not penetrate into hydrogen-rich layers, the helium layer expands, and much, if not most, of the accreted matter is lost during the event because of the interaction of the expanded envelope with the companion star.

Analysis of the results suggests that it is unlikely that, in the real world, a hydrogen-accreting CO white dwarf with a typical initial mass will attain the Chandrasekhar mass. Dynamical helium-burning flashes are probable.

Subject headings: accretion, accretion disks — novae, cataclysmic variables — nuclear reactions, nucleosynthesis, abundances — stars: interiors — supernovae: general — white dwarfs

1. INTRODUCTION

The accretion of hydrogen-rich matter onto white dwarfs, apart from being responsible for classical and symbiotic nova outbursts, has been suggested as being responsible for Type Ia supernovae (SNe Ia; Whelan & Iben 1973). The apparent absence of hydrogen lines in spectra of SNe Ia, which does not necessarily imply the complete absence of hydrogen in the presupernova system, has, nevertheless, motivated the search for progenitor systems in which hydrogen has been lost during prior evolution.

One scenario that has emerged from this search consists of a primordial system of two intermediate mass stars that evolve through a series of common envelope episodes into a final system of two very close carbon-oxygen (CO) white dwarfs of combined mass larger than the Chandrasekhar mass (Iben & Tutukov 1984; Webbink 1984). Angular momentum loss by gravitational wave radiation leads to a merger of the white dwarfs and to a possible star-disrupting explosion.

Although there are several theoretical difficulties at various steps of the process (e.g., the need for a free parameter to define the separation of the two stars after a common envelope episode, and the possibility that carbon burns quiescently in the merger product that then experiences core collapse instead of explosion; see the discussion in Mochkovich & Livio 1990), it has been the lack of observed appropriately massive close white dwarf pairs that has caused the most widespread doubts about the merger scenario (Robinson & Shafter 1987; Bragaglia et al. 1990). The discovery by Marsh and his collaborators (Marsh 1995; Marsh, Dhillon, & Duck 1995) of five close helium white dwarf pairs, several of which are close enough to merge in less than a Hubble time, removes the doubt that close white dwarf pairs occur in nature, and scenario modeling shows that the number of observed close white dwarf pairs (now eight) must be at least quadrupled before the supposition that suitably massive close CO white dwarf pairs occur in nature is seriously challenged (Iben, Tutukov, & Yungelson 1997).

Nevertheless, in recent years, the search for possible progenitors of SNe Ia has focused on CO white dwarfs accreting hydrogen from a companion with a hydrogen-rich envelope. Two popular candidate systems are long period cataclysmic variables (CVs) and supersoft X-ray binaries (van den Heuvel et al. 1992) in which accretion rates are large enough that hydrogen burning proceeds through a series of mild flashes or burns at a steady rate equal to the accretion rate.

It is possible to obtain a thermonuclear explosion that delivers some 10^{51} ergs without the requirement that the mass of the exploding system exceed the Chandrasekhar mass. This is the case, for example, when the total mass of a white dwarf accreting helium at an appropriate rate exceeds $\sim$0.65–0.8 $M_\odot$ (Nomoto & Sugimoto 1977). If helium is accreted onto a very cold CO white dwarf at the rate $\sim 3 \times 10^{-8}$ $M_\odot$ yr^{-1}, a violent explosion occurs after the accretion of $\Delta M_{\rm He} \sim 0.15$ $M_\odot$, nearly independent of the initial mass of the underlying white dwarf (Iben & Tutukov 1991). The critical amount of accreted helium depends strongly on the accretion rate, with $\Delta M_{\rm He} > 0.4$ $M_\odot$ for an

[1] Dipartimento di Fisica, Università de L'Aquila, Via Vetoio, 67100 L'Aquila, Italy; cassisi@axscaq.aquila.infn.it.
[2] Osservatorio Astronomico di Teramo, Via M. Maggini 47, 64100 Teramo, Italy; tornambe@astrte.te.astro.it.
[3] Astronomy and Physics Departments, University of Illinois, 1002 West Green Street, Urbana, IL 61801; icko@astro.uiuc.edu.

accretion rate of $\sim 5 \times 10^{-9}\ M_\odot\ \mathrm{yr}^{-1}$ (Limongi & Tornambè 1991). If the white dwarf is initially cold enough and massive enough, helium burning can evolve into a detonation, and an inward moving compression wave can then lead to the detonation of carbon in the core (Tutukov & Khokhlov 1992; Woosley & Weaver 1994).

The development of a critical helium layer above a CO core can be a consequence of the burning of accreted hydrogen-rich matter, as well as of the direct accretion of helium from a helium companion star. In this paper, we focus on the first of these two possibilities. The mass of the critical helium layer and the violence of the explosion differ in the two cases because of the injection of energy from hydrogen burning into the accreted layer.

In the case of hydrogen-accretion rates near to or larger than the Eddington limit, it is well known that the accreted matter will form an expanded configuration, typical of a red giant star (e.g., Nomoto, Nariai, & Sugimoto 1979; Iben 1988). As the accretion rate is lowered, a range of accretion rates is encountered where hydrogen is burned at the base of the accreted layer at the same rate as it is accreted. Lowering the accretion rate still further, a zone is encountered where recurrent hydrogen shell flashes take place. The accretion rate at the borderline between steady state burning and flashing behavior decreases as the mass of the white dwarf is decreased (see, e.g., Fig. 2 in Iben 1982). As the accretion rate is lowered below the borderline, flashes become stronger and stronger, changing from mild, non-dynamical, events to strong, nova-like outbursts. The precise values of the accretion rate that separate the various zones and the long-term evolution of the accreting dwarf have yet to be worked out in adequate detail.

The pioneering works of Giannone & Weigert (1967), Starrfield, Sparks, & Truran (1974a, 1974b), and others followed only one cycle prior to a thermonuclear outburst. Detailed computations that followed several recurrent and mild hydrogen shell flashes were first conducted, we believe, by Paczyński & Żytkow (1978), who studied behavior as a function of accretion rate, including rates that lead to steady state hydrogen burning. In the Paczyński & Żytkow work, and in similar work by others (e.g., Sion, Acierno, & Tomczyk 1979; Sion & Starrfield 1986; and Livio, Prialnik, & Regev 1989), no particular attention was paid to the consequences of building up a helium layer. Iben (1982) carried the evolution of one model to the ignition of a helium shell flash, but a systematic study of the long-term evolution of hydrogen-accreting white dwarfs as a function of accretion rate did not appear until the work of José, Hernanz, & Isern (1993) who used a semianalytical code in plane-parallel geometry to study evolution through a large number of hydrogen shell flashes and also some consequent helium shell flashes. Their choice of geometry considerably simplifies the analysis of long-term behavior, but results in the loss of some important details.

In the present work, the long-term evolution of hydrogen-accreting white dwarfs is followed with a spherically symmetric quasi-static code. Input physics, numerical techniques, and assumptions are given in § 2, where the results of the evolutionary sequences are also presented. In § 3 the mass of the helium layer when a helium shell flash is initiated is shown to be smaller, all other things being equal, in a helium-accreting model than in a hydrogen-accreting model. A discussion of the results is given in § 4, and conclusions are given in § 5.

2. INPUT PHYSICS AND NUMERICAL TECHNIQUES

An updated version of the FRANEC code (Chieffi & Straniero 1989) has been employed both to produce initial cold white dwarf models and to conduct the hydrogen-accretion experiments. Most of the departures from the original code are in the reaction rates, which have been taken from Caughlan & Fowler (1988), except for the $C^{12}(\alpha, \gamma)O^{16}$ reaction rate, which is taken from Caughlan et al. (1985). The method for solving the nuclear reaction network is the same as that used by Chieffi, Limongi, & Straniero (1998; see also Limongi et al. 1994), and the method of computing accretion is the same as that used by Limongi & Tornambè (1991).

An initial white dwarf model of mass $0.516\ M_\odot$ has been generated by first evolving a horizontal-branch model of solar metallicity until it reaches the early asymptotic giant branch (EAGB) phase, whereupon modest mass loss is employed and evolution is continued until the model departs from the EAGB and evolves into a white dwarf (Castellani, Limongi, & Tornambè 1992). Thus, the dimensions and chemical profile of the helium layer and of the hydrogen envelope, as well as those of the CO core, are realistic. An initial white dwarf model of mass $0.8\ M_\odot$ has been produced by evolving without mass loss a helium star constructed by Limongi & Tornambè (1991).

When the white dwarf models reach a luminosity $L \sim 10^{-3}\ L_\odot$, matter of composition $X = 0.70$, $Y = 0.28$ and solar metallicity (in the Ross & Aller 1976 distribution) is accreted onto the models at the rate $\dot{M} = 10^{-8}\ M_\odot\ \mathrm{yr}^{-1}$. The first hydrogen shell flash is very strong, and the models are evolved through the flash with extremely short time steps and infrequent rezoning. Once through the first flash, computations proceed smoothly and the only remaining problem is the requirement for large quantities of computer time. Subsequent accretion experiments begin with the white dwarf models whose outer layers have been heated by the first flash.

2.1. *Accretion of Hydrogen-rich Matter onto a* CO *White Dwarf of Initial Mass* $0.516\ M_\odot$

After the first flash, accretion onto the CO white dwarf of mass $0.516\ M_\odot$ is taken at the rates 2×10^{-8}, 4×10^{-8}, 6×10^{-8}, 10^{-7}, and $10^{-6}\ M_\odot\ \mathrm{yr}^{-1}$. Since many models experience recurrent hydrogen shell flashes, it is worth summarizing briefly the main features of a typical flash before describing in detail the long-term effect of mass accretion.

As shown in Figure 1, a model describes a loop in the Hertzsprung-Russell (H-R) diagram during each pulse cycle. Between points A and B, the efficiency of hydrogen burning drops steadily from $L_H/L_{tot} \sim 1$ to a minimum value of ~ 0.1. During this portion of the cycle, the evolutionary timescale is rather long, and the model accretes a substantial fraction (around half) of the matter that is accreted between the onset of two successive hydrogen shell flashes. As L_H/L_{tot} decreases, helium-burning reactions (mostly the 3α process) try to support the structure, and L_{He} reaches a relative maximum (which is usually a small fraction of the total luminosity). The main contribution to the surface luminosity comes from the release of gravothermal energy.

After point B, the hydrogen-burning rate increases and burning evolves very soon into a rather powerful flash (point C). The maximum hydrogen-burning luminosity is reached at point D. The evolutionary timescale becomes

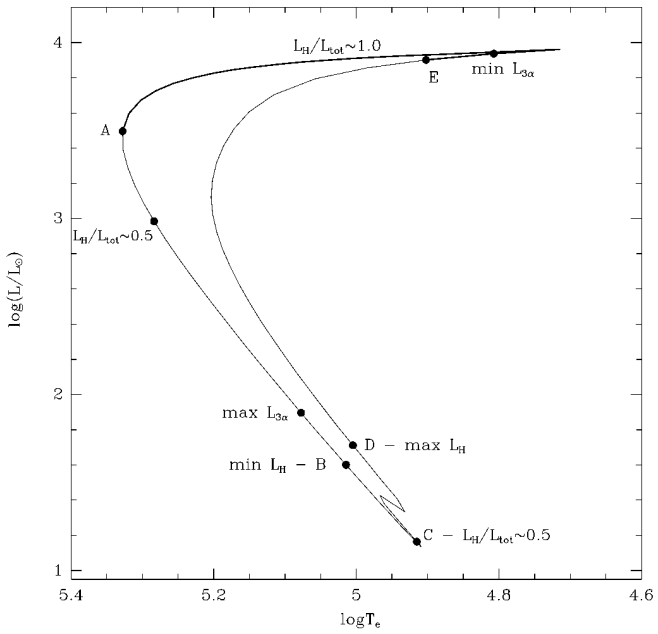

FIG. 1.—Evolution in the Hertzprung-Russell (H-R) diagram of a white dwarf accreting hydrogen-rich matter during a typical hydrogen-burning flash. The various letters mark selected evolutionary points (see text).

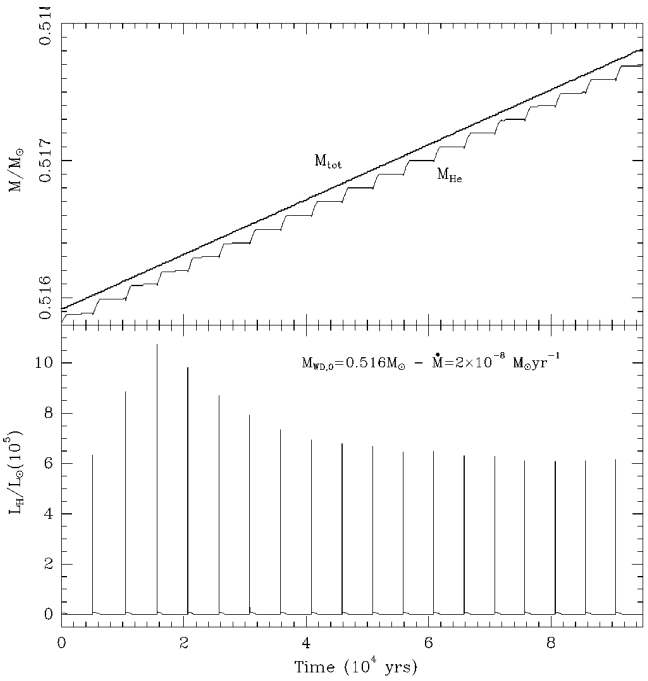

FIG. 2.—Time dependence of several characteristics of a model of initial mass $M_{WD,0} = 0.516\ M_\odot$ accreting hydrogen-rich matter at the rate $\dot{M} = 2 \times 10^{-8}\ M_\odot\ \mathrm{yr}^{-1}$. The origin of the temporal scale is arbitrarily fixed. (*Top panel*) The total mass M_{tot} and the location in mass M_{He} of the outer edge of the helium layer. (*Bottom panel*) The hydrogen-burning luminosity L_H.

very small, as external layers expand rapidly in an attempt to return to a quiescent burning regime. This is achieved at point E where, finally, L_H/L_{tot} again becomes of the order of unity. As evolution progresses, the mass above the center of the hydrogen-burning shell decreases and, in consequence, the model evolves to the blue in the H-R diagram. Over the interval E–A, $L_H/L_{tot} \sim 1$, as the model accretes the other approximately half of the matter accreted over the entire cycle. The exact location of the various reference points, as well as the shape of the cycle in the H-R diagram, depends, of course, on both the accretion rate and the mass of the underlying white dwarf. For a given white dwarf mass, the higher the accretion rate, the smaller is the excursion to the red at high luminosity in the H-R diagram.

A model accreting at the rate $\dot{M} = 2 \times 10^{-8}\ M_\odot\ \mathrm{yr}^{-1}$ enters very quickly into a recurrent mild flash regime. In 10 cycles the model acquires asymptotic pulse characteristics (light curve, minimum and maximum values of total luminosity, nuclear and gravothermal energy-production rates, effective temperature, density and temperature in the hydrogen-burning shell, etc.). In all, 19 complete pulses have been followed. In Figure 2, the total mass and the mass of the hydrogen-exhausted core, as well as the hydrogen-burning luminosity, are plotted as functions of time. The

TABLE 1

QUANTITIES FOR STELLAR MODELS EXPERIENCING HYDROGEN-BURNING PULSES

$\dot{M}$[a] ($M_\odot\ \mathrm{yr}^{-1}$)	Period[b] (yr)	log ($L_{max}/L_\odot$)[c] ($L_\odot$)	log ($L_{min}/L_\odot$)[d] ($L_\odot$)	$L_H^{max}/L_\odot$[e] ($L_\odot$)	$L_H^{min}/L_\odot$[f] ($L_\odot$)
$M_{WD,0} = 0.516\ M_\odot$					
2×10^{-8}.....	5.375×10^3	3.960	1.137	6.5×10^5	2.45
4×10^{-8}.....	1.812×10^3	4.158	1.597	7.0×10^5	6.22
$M_{WD,0} = 0.80 M_\odot$					
10^{-8}[g].....	3.111×10^3	4.397	0.960	1.4×10^7	0.19
4×10^{-8}.....	4.825×10^2	4.389	1.657	2.6×10^6	2.77
10^{-7}	2.042×10^2	4.341	2.188	4.4×10^5	25.1

NOTE.—Selected theoretical evolutionary quantities for stellar models experiencing hydrogen-burning pulses (see text) for two different values of the initial mass of the accreting white dwarf and for various accretion rates.

[a] Accretion rate.
[b] Time between successive hydrogen pulses after an asymptotic regime has been achieved.
[c] Maximum logarithmic luminosity of the star during the hydrogen-pulse cycle.
[d] Minimum logarithmic luminosity of the star during the hydrogen-pulse cycle.
[e] Maximum value of the hydrogen-burning luminosity during a pulse.
[f] Minimum value of the hydrogen-burning luminosity during a pulse.
[g] Quantities are estimated from results for two pulses.

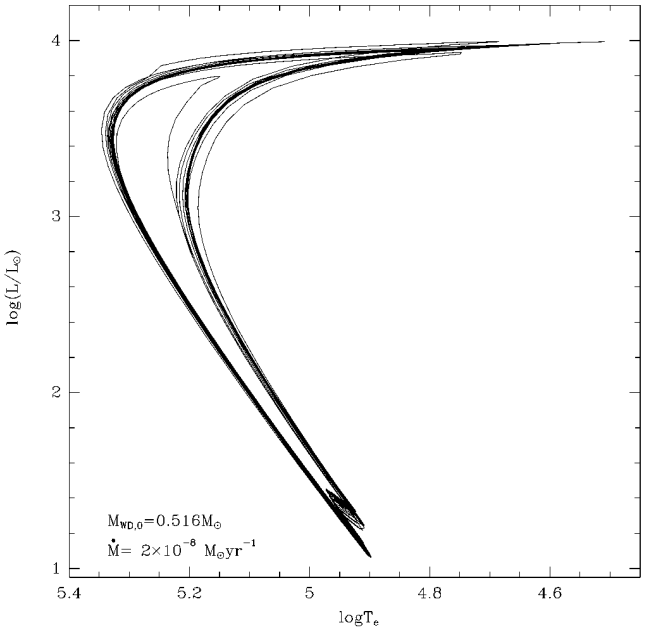

FIG. 3.—Evolution in the H-R diagram for the model with $M_{\rm WD,0} = 0.516\,M_\odot$ and $\dot{M} = 2 \times 10^{-8}\,M_\odot\ {\rm yr}^{-1}$.

evolutionary track of the model is shown in Figure 3. The computations have been terminated well before any appreciable effect occasioned by the growing mass of the helium layer appears. The possible long-term evolution of this model will be discussed in § 3. Tables 1 and 2 report some major physical quantities once the asymptotic pulsing regime has been attained.

When $\dot{M} = 4 \times 10^{-8}\ M_\odot\ {\rm yr}^{-1}$, the evolution is quite different. In fact, the model soon enters a steady state configuration in which the accreted matter is burned at the same rate as it is deposited on the surface of the white dwarf. The existence of this steady state configuration follows also from the behavior of models that experience hydrogen shell flashes. That is, when the accretion rate is such that hydrogen shell flashes occur, there is a portion of the pulse cycle during which the only active energy source is hydrogen burning ($L_{\rm H}/L_{\rm tot} = 1$, $L_{\rm grav} \sim 0$). The rate at which hydrogen is consumed is precisely proportional to $L_{\rm H}$, so, if at any point along the $L_{\rm H}/L_{\rm tot} = 1$ portion of the cycle, hydrogen is added at the same rate as it is consumed, the model will not change its physical characteristics except on the long timescale associated with the change in mass of the hydrogen-exhausted core. In the case at hand, the initial steady state model is characterized by $\log L \sim 3.5$, $\log T_e \sim 5.35$. The main physical characteristics of the model remain almost unchanged until a total mass of $0.594\ M_\odot$ has been achieved. At this point, in order to maintain a steady state, a higher accretion rate would have to be chosen. At the fixed accretion rate of $\dot{M} = 4 \times 10^{-8}\ M_\odot\ {\rm yr}^{-1}$, recurrent mild hydrogen shell flashes (pulses) commence. After about 19 pulse cycles, the pulse characteristics approach asymptotic values. Some of the major physical characteristics of the pulses, once the asymptotic regime has been attained, are reported in Tables 1 and 2. The evolution of the model in the HR diagram is shown in Figure 4, where the very small region traversed by the steady state models is the nearly horizontal line pointed to by an arrow. The time-dependent behavior of the hydrogen- and helium-burning luminosities during the hydrogen-pulse evolutionary phase is plotted in Figure 5. When making comparisons to other models, it is important to keep in mind that the model mass is now $\gtrsim 0.6\ M_\odot$, significantly larger than the initial mass of $0.516\ M_\odot$.

The evolution of the pulsating model has been followed for an additional 49 pulses during the asymptotic regime until helium burning becomes important. During the entire evolution (steady state burning plus the hydrogen-pulse phase), the mass of the helium layer (defined as the region within which the abundance by mass of helium is ≥ 0.5) increases from an original value of $4.3 \times 10^{-4}\ M_\odot$ to a final value of $0.0934\ M_\odot$.

At the end of the 68th hydrogen pulse, near where $L_{\rm H}/L_{\rm tot}$ attains its minimum value (~ 0.1), a powerful helium shell

TABLE 2

QUANTITIES FOR STELLAR MODELS EXPERIENCING A HELIUM SHELL FLASH

$\dot{M}$[a] ($M_\odot\ {\rm yr}^{-1}$)	$M_{\rm WD}^{\rm fin}$[b] ($M_\odot$)	$L_{\rm He}^{\rm max}/L_\odot$[c] ($L_\odot$)	$M_{\rm H}^{\rm env}$[d] ($M_\odot$)	$\log T_{\rm shell}^{\rm He}$[e] (K)	$\log \rho_{\rm shell}^{\rm He}$[f] (g cm^{-3})	H Mixing[g]
$M_{\rm WD} = 0.516\ M_\odot$						
4×10^{-8}[h].....	0.6094	5.48×10^{11}	9×10^{-5}	8.490	5.008	Yes
6×10^{-8}.....	0.5975	2.29×10^{11}	6×10^{-5}	8.537	4.625	Yes
10^{-7}[h]	0.5778	1.56×10^{10}	14×10^{-5}	8.457	4.642	Yes
$M_{\rm WD,0} = 0.80\ M_\odot$						
10^{-7}	0.8105	4.17×10^{10}	2×10^{-5}	8.601	4.390	No
1.6×10^{-7}.....	0.8106	4.33×10^{10}	1×10^{-5}	8.608	4.371	No

NOTE.—Selected theoretical evolutionary quantities for stellar models experiencing a helium shell flash after the mass-accretion episode for two different values for the initial mass of the accreting white dwarf

[a] Accretion rate.
[b] Final mass of the accreting white dwarf.
[c] Helium-burning luminosity at the end of the computation.
[d] Mass of the hydrogen-rich envelope.
[e] Logarithmic temperature at the base of the He shell at the peak of the helium shell flash.
[f] Logarithmic density at the base of the helium shell at the peak of the helium-burning shell flash.
[g] Information about the occurrence of mixing between the hydrogen-rich envelope and the helium convective shell.
[h] Quantities pertain to the last computed model.

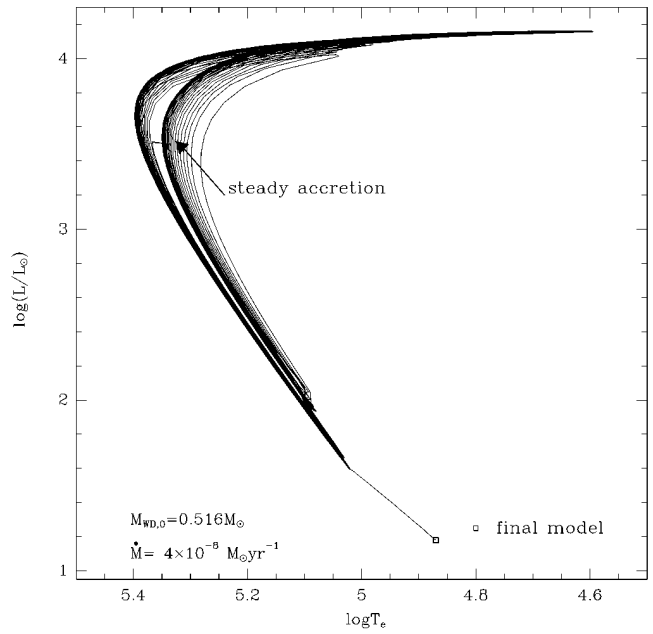

FIG. 4.—Evolution in the H-R diagram for the model with $M_{WD,0} = 0.516\,M_\odot$ and $\dot{M} = 4 \times 10^{-8}\,M_\odot\ \mathrm{yr}^{-1}$.

flash develops (see the far right portion of Fig. 5*b*). Convection spreads quickly over the entire helium layer. Most of the energy produced by the helium-burning reactions is used up locally in removing electron degeneracy. External layers expand slightly, and the surface luminosity drops slightly (log L decreases from 1.6 to 1.2). The flash has been followed until $L_{\mathrm{He}} \sim 5.44 \times 10^6\ L_\odot$. Computations have been terminated at this point because the outer edge of the helium convective layer reaches the inner edge of the hydrogen-rich envelope, necessitating the use of a time-dependent mixing algorithm.

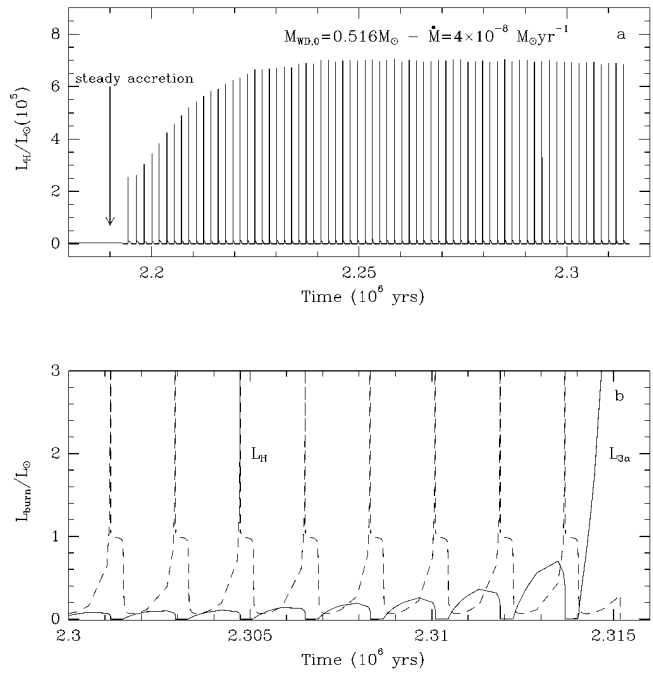

FIG. 5.—Time-dependence of the hydrogen-burning luminosity L_{H} during the steady state burning and pulsing phases (*top panel*) and of L_{H} and the helium-burning luminosity L_{He} during the last part of the pulsing phase up to the helium-burning thermonuclear runaway for the model described in Fig. 4.

A comparison to the models of Woosley & Weaver (1994, in particular, models 5 and 9 in their Table 1) suggest that our model will escape becoming a sub-Chandrasekhar supernova. It should be noted, however, that their models 5 and 9 ignite helium well above the base of the helium layer while, in our model, helium ignition occurs at the bottom of the helium layer. In addition, their model 9 attains a maximum temperature of $\sim 0.85 \times 10^8$ K, whereas ours is already at 3×10^8 K when computations have been terminated, and there is no indication that the temperature is near a maximum. An added complication is that, in our case, protons will diffuse into the helium convective layer until they reach temperatures high enough for hydrogen to burn. The calculations of Hollowell, Iben, & Fujimoto (1990) and of Iben & MacDonald (1995), show that the entropy added by hydrogen burning forces the formation of a new convective shell that is detached from the first one and mixes to the surface matter that has experienced partial helium burning followed by hydrogen burning. Were it not for the presence of a close companion, the real analog of the model would expand to giant dimensions. The presence of a close companion leads to common envelope action with the loss of the hydrogen-rich envelope and probably most of the helium layer.

The evolution of a model of initial mass $0.516\ M_\odot$ that accretes at the rate $6 \times 10^{-8}\ M_\odot\ \mathrm{yr}^{-1}$ differs from that of the previous two models in that a regime of mild hydrogen shell flashing is not encountered before a strong helium shell flash occurs. The phase of steady state hydrogen burning takes place at constant luminosity ($\log L/L_\odot \sim 3.71$) and nearly constant effective temperature ($\log T_e \sim 5.37$). When a total mass of about $0.597\ M_\odot$ has been achieved, the helium-burning reactions are ignited at the base of the helium layer, and the burning develops rapidly into a flash that supports a growing convective layer. The helium-burning luminosity reaches a maximum of $L_{\mathrm{He}} \sim 2.28 \times 10^6\ L_\odot$ and thereafter declines. The convective layer continues to grow in mass as L_{He} decreases, and its outer edge eventually enters into hydrogen-rich layers. At this point calculations have been terminated, but, once again, one may anticipate diffusion of hydrogen into the helium-rich convective layer until hydrogen ignites and forms a detached convective shell that extends to the surface. And, once again, the model envelope will expand to giant dimensions, leading in the real world to the loss of the hydrogen-rich envelope and most of the helium layer.

A model of initial mass $0.516\ M_\odot$ that accretes at the rate $\dot{M} = 10^{-7}\ M_\odot\ \mathrm{yr}^{-1}$ reaches the steady state hydrogen-burning phase when $\log L/L_\odot \sim 3.86$ and $\log T_e \sim 5.0$. Although the luminosity remains almost constant during further accretion, the model at first expands and evolves slowly to the red, but, when the mass of accreted matter reaches $\sim 0.01\ M_\odot$, the model evolves back to the blue toward a nearly fixed accumulation point ($\log T_e \sim 5.04$). When the total mass of the model reaches $0.578\ M_\odot$, a helium shell flash develops. This time, the maximum helium-burning luminosity is $L_{\mathrm{He}} \sim 1.58 \times 10^5\ L_\odot$. Again, the convective layer continues to grow in mass until its outer edge reaches and ingests hydrogen-rich matter.

It interesting that, in the two models of largest accretion rate, the maximum temperature inside the helium layer is not initially located at the base of the layer itself. In the $\dot{M} = 8 \times 10^{-8}\ M_\odot\ \mathrm{yr}^{-1}$ case, it moves to the base after about 90% of the total evolutionary time has elapsed, while in the $\dot{M} = 10^{-7}\ M_\odot\ \mathrm{yr}^{-1}$ case, it moves to the base just prior to the full development of the helium shell flash.

The model with $\dot{M} = 10^{-7}\ M_\odot\ \mathrm{yr}^{-1}$ is initially at the borderline between models that can burn at a steady rate at fixed luminosity and nearly fixed surface temperature and those that evolve into red giants. To illustrate the phenomenon of evolution into a red giant, we have computed a model of initial mass 0.516 $M_\odot$ that accretes at the rate $\dot{M} = 10^{-6}\ M_\odot\ \mathrm{yr}^{-1}$. In only 100 yr, the model reaches the Hayashi track (log $T_e \sim 3.5$). Accretion is continued for another 1.64×10^5 yr until a model mass of $\sim 0.68\ M_\odot$ and radius $\sim 750\ R_\odot$ have been achieved. During this time, hydrogen continues to burn at a nearly constant rate determined by the mass of the hydrogen-exhausted core, which has increased by only $\sim 0.016\ M_\odot$ over the period studied.

2.2. *Accretion of Hydrogen-rich Matter onto a* CO *White Dwarf of Initial Mass* 0.8 $M_\odot$

The preheated CO white dwarf model of mass 0.8 $M_\odot$ has been subjected to accretion of hydrogen-rich matter at the rates 10^{-8}, 4×10^{-8}, 10^{-7}, 1.6×10^{-7} and 4×10^{-7} $M_\odot\ \mathrm{yr}^{-1}$. For $\dot{M} = 10^{-8}\ M_\odot\ \mathrm{yr}^{-1}$, hydrogen burns via recurrent pulses, but numerical difficulties during the second hydrogen shell flash have prevented us from exploring the asymptotic properties of the pulses. Indeed, this model is very near the borderline for the occurrence of strong pulses as defined by Iben (1982). The large radii attained by the model during its evolution (as far as we have followed it) suggests that, in a close binary, mass loss from the system due to Roche-lobe overflow and common envelope action would be extensive and make the accretion process very inefficient (in the sense that a large fraction of the matter accreted between hydrogen shell flashes is lost during the large radius portion of the pulse cycle).

For $\dot{M} = 4 \times 10^{-8}\ M_\odot\ \mathrm{yr}^{-1}$, the model settles into a mild recurrent hydrogen-flash regime, behaving in a fashion similar to that of models of the same class described in § 2.1. Computations are followed until pulse characteristics achieve the asymptotic values given in Tables 1 and 2.

Recurrent mild hydrogen shell flashes occur also when $\dot{M} = 10^{-7}\ M_\odot\ \mathrm{yr}^{-1}$. This time, evolution has been followed through several hundred hydrogen-burning pulse episodes, until helium burning accelerates into a thermonuclear runaway. Actually, the rate of helium burning oscillates with steadily increasing amplitude during the entire experiment, as illustrated in Figure 6, which shows the time dependence of the hydrogen- and helium-burning luminosities over a small time interval. As shown in Figure 7, a true helium shell flash, modified as it is first getting underway by the occurrence of a hydrogen shell flash, begins after $\sim 6.46 \times 10^4$ yr of accretion.

A small convective layer supported by helium burning appears before, and survives the interruption by the hydrogen shell flash. However, the outer edge of the convective layer never reaches hydrogen-rich matter before it recedes. On the other hand, the entire helium envelope expands to red giant dimensions. Thus, in the real analog in a close binary system, a large fraction of the helium envelope is lost from the system when the accretor fills its Roche lobe, thus considerably lowering the efficiency at which the CO core can grow secularly in mass.

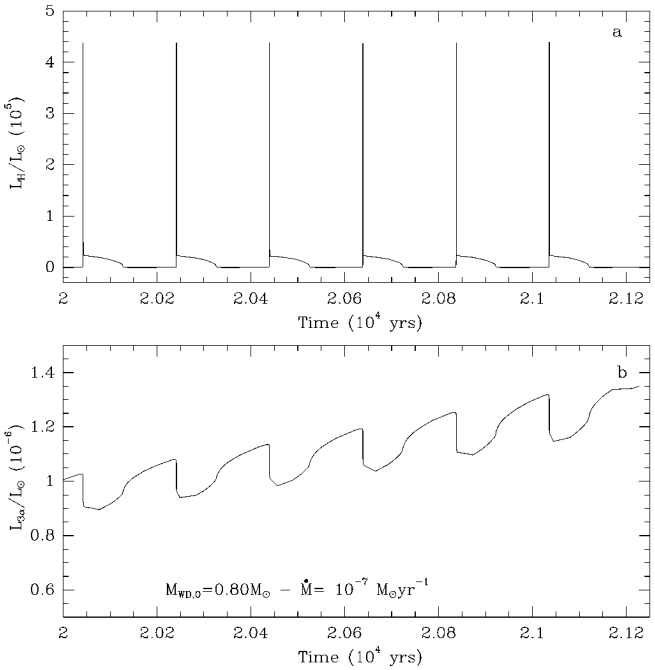

FIG. 6.—Evolution with time of L_H (*top panel*) and of L_{He} (*bottom panel*) during the recurrent shell hydrogen-pulsing phase when $M_{WD,0} = 0.8\ M_\odot$ and $\dot{M} = 10^{-7}\ M_\odot\ \mathrm{yr}^{-1}$.

For $\dot{M} = 1.6 \times 10^{-7}\ M_\odot\ \mathrm{yr}^{-1}$, an initial rapid excursion of the model toward the region of red giants shows that the model is at the borderline of the stationary burning and the red giant regimes of accretion. After only a very small amount of mass ($\sim 6.8 \times 10^{-4}\ M_\odot$) has been accreted, the model evolves back to the blue and settles at log $L/L_\odot \sim 4.06$ and log $T_e \sim 5.6$, where it remains until its total mass reaches $\sim 0.8106\ M_\odot$. At this point, a helium shell flash develops, but, as in the $\dot{M} = 10^{-7}\ M_\odot\ \mathrm{yr}^{-1}$ case, the outer edge of the convective shell does not reach the base of the hydrogen-rich envelope. Following the initial helium flash, helium burning continues quiescently, and the model envelope expands until the model radius reaches $\sim 560\ R_\odot$.

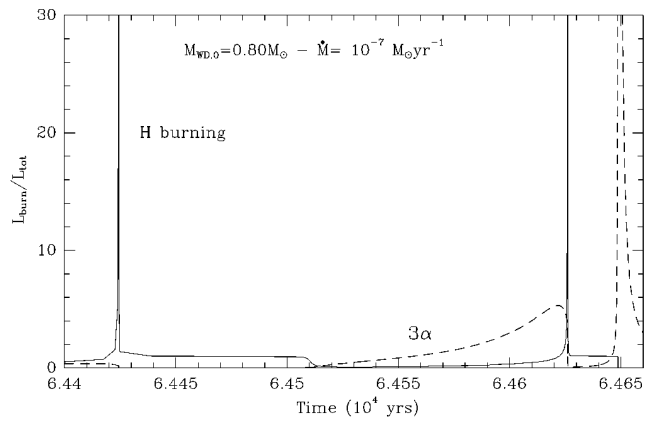

FIG. 7.—Evolution with time of L_H and L_{He} during the last computed portion of the evolution of the model described in Fig. 6.

Once again, one can anticipate that, in a close binary, mass loss from the system dramatically lowers the efficiency with which the CO core increases secularly in mass.

For $\dot{M} = 4 \times 10^{-7}\ M_\odot\ \mathrm{yr}^{-1}$, the model becomes an AGB star with a hydrogen-rich envelope that increases steadily in mass, exactly as in the case of the model of initial mass 0.516 $M_\odot$ accreting at the rate $\dot{M} = 10^{-6}\ M_\odot\ \mathrm{yr}^{-1}$ (§ 2.1).

3. COMPARISON TO HELIUM-ACCRETING MODELS

As noted earlier by José et al. (1993), the occurrence of hydrogen burning reduces the amount of matter that must be accreted before a helium shell flash is initiated relative to the amount needed when pure helium is accreted. Simply put, the energy released by hydrogen burning is much larger than that released by the gravothermal source in the absence of hydrogen burning; thus, the helium layer is maintained at a higher temperature and helium ignition occurs sooner when hydrogen is contained in the accreted matter (see also the discussion of Fig. 15 in Iben & Tutukov 1996). As a corollary, all other things being equal, the strength of the helium shell flash is smaller when hydrogen-rich material is accreted.

To show this property in more detail, we have performed an additional experiment in which hydrogen-free matter consisting of helium (abundance by mass $Y = 0.98$) and elements heavier than helium (abundance by mass $Z = 0.02$) is accreted at the rate $\dot{M} = 4 \times 10^{-8}\ M_\odot\ \mathrm{yr}^{-1}$ onto the original cool model of mass $M_{\mathrm{WD},0} = 0.516\ M_\odot$. In Figure 8, the structure of the helium-accreting model is compared in the ρ-T plane to the structure of the hydrogen-accreting model of the same initial mass and accretion rate (§ 2.1) at a time when both models are of mass 0.6045 $M_\odot$; a helium shell flash is about to begin in the hydrogen-accreting model. It is evident that the helium layer is maintained at a higher temperature in the hydrogen-accreting model than in the helium-accreting model, with the consequence that the helium-accreting model must develop a significantly more massive helium layer before experiencing a helium shell flash.

This is demonstrated explicitly in Figure 9, where the maximum temperature T_{max} in the interior during the interpulse phase, and the temperature T_{Heshell}, where the rate of energy generation by helium burning is at a maximum, are shown for the two models as functions of model mass (or, equivalently, as functions of time). The occurrence of a helium shell flash is marked by the nearly vertical rise in temperature after the convergence of the T_{max} and T_{Heshell} curves. Prior to the helium shell flash, the relevant temperatures in the hydrogen-accreting model are always larger than those of the helium-accreting model. When the flash begins, the mass of the helium layer in the helium-accreting model is $\Delta M_{\mathrm{He}} \sim 0.128\ M_\odot$, which is $\sim 0.035\ M_\odot$ or 37% larger than ΔM_{He} for the hydrogen-accreting model.

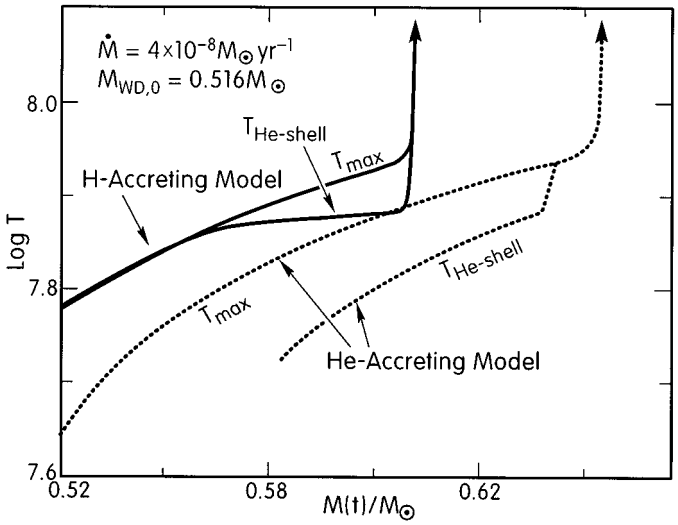

FIG. 9.—Behavior of the maximum internal temperature T_{max} and of the temperature in the helium-burning shell (at the point where the rate of helium burning is at a maximum) as a function of model mass for the hydrogen- and helium-accreting models described in Fig. 9.

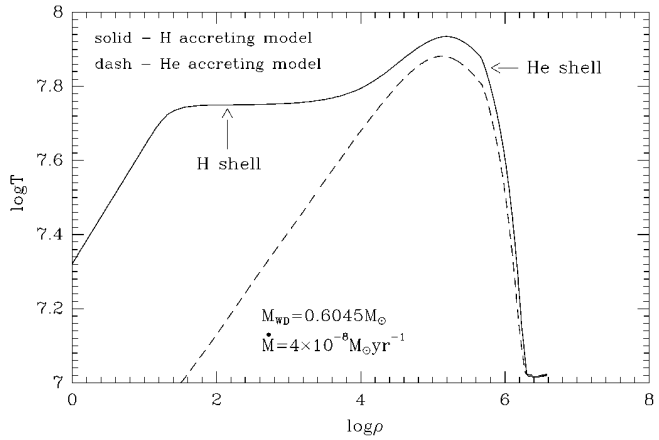

FIG. 8.—Structure in the ρ-T plane of a model accreting helium at the rate $4 \times 10^{-8}\ M_\odot\ \mathrm{yr}^{-1}$ and of a model accreting hydrogen-rich matter at the same rate. Both models have the same mass, 0.6045 $M_\odot$, and both derive from the same initial CO white dwarf model of mass 0.516 $M_\odot$.

Computations of the helium-accreting model have been terminated when the outer edge of the convective shell sustained by helium-burning fluxes reaches the photosphere. At this point, the time step needed to obtain model convergence has dropped below 1 s, and the timescale for nuclear energy release is less than the mixing time in the convective shell.

In the hydrogen-accreting model during the steady state burning regime, both T_{max} and T_{Heshell} are larger than the temperature T_{Hshell} at the center of the hydrogen-burning shell, which remains almost constant. During the hydrogen-pulsing phase, the energy released in a shell flash heats matter for several density scale heights in either direction beyond the center of the burning shell, but expansion of matter below the burning region leads to cooling. As the hydrogen-burning luminosity dies down, thermal energy continues to flow inward (as well as outward, of course) from the hydrogen-burning shell, but most of the reheating of the helium layer is due to the release of gravothermal energy as the helium layer recontracts. That is, during the flash, the rapid injection of nuclear energy leads to overpressures and expansion against gravity; energy is stored in the form of gravitational potential energy. After the flash dies down, the stored energy is released with interest to reheat the helium layer. In any case, the net result during both the steady state burning and pulsing phases is that the mean temperature in the helium layer is maintained at a

higher value in the hydrogen-accreting model than in the helium-accreting model of the same mass and accretion rate.

A comparison of the model with $M_{\rm WD} = 0.8\ M_\odot$ and $\dot{M} = 10^{-7}\ M_\odot\ {\rm yr}^{-1}$ discussed in § 2.2 and a helium-accreting model of the same initial mass and accretion rate computed by Limongi & Tornambè (1991) discloses an additional property: the difference in $\Delta M_{\rm He}$ at helium ignition between a helium-accreting model and a hydrogen-accreting model increases with increasing $M_{\rm WD,0}$. The reason for this is that the larger the core mass, the larger is the mean hydrogen-burning luminosity, and the more effective is hydrogen burning in keeping the helium layer hot; the hotter the helium layer, the smaller is the mass of the helium layer when the helium shell flash occurs.

4. DISCUSSION OF THE RESULTS

Figure 10 summarizes the results and describes schematically the outcomes encountered for the various models discussed in § 2. The abscissa gives the initial mass of the accreting white dwarf, and the ordinate gives the logarithm of the accretion rate in $M_\odot\ {\rm yr}^{-1}$. A regime involving recurrent hydrogen-burning pulses is represented by a saw-tooth symbol. A regime in which hydrogen is burned as rapidly as it is accreted (giving rise to a helium layer of steadily increasing mass) is represented by a continuous line. The occurrence of a helium shell flash is marked with a large filled circle. In one case ($\dot{M} = 4 \times 10^{-8}\ M_\odot\ {\rm yr}^{-1}$, $M_{\rm WD,0} = 0.516\ M_\odot$), a phase of recurrent hydrogen pulses follows a phase of steady state burning. In another case ($\dot{M} = 10^{-7}\ M_\odot\ {\rm yr}^{-1}$, $M_{\rm WD,0} = 0.8\ M_\odot$), the helium shell flash occurs at the end of a recurrent hydrogen-pulse phase that is not preceded by a steady state burning phase. Finally, the positions in the $\dot{M}$-$M_{\rm WD}$ plane of models that quickly develop an envelope of red giant dimensions are marked by symbols consisting of a dot inside a circle.

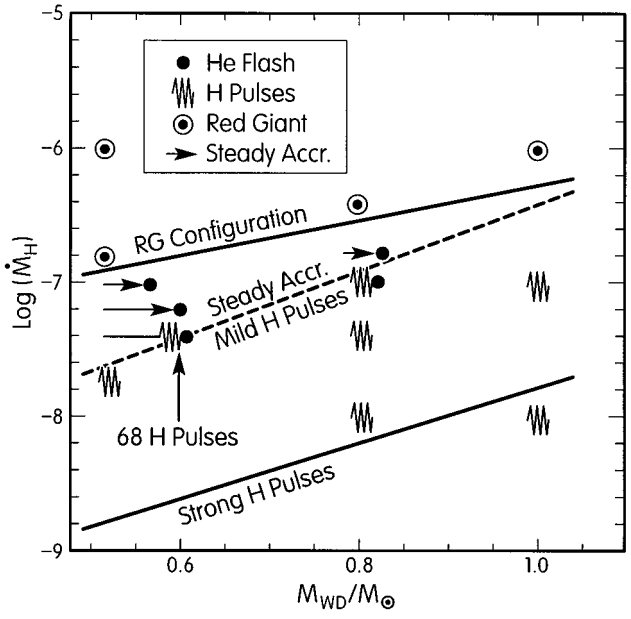

FIG. 10.—Parameter space in the $\dot{M}$-$M_{\rm WD}$ plane explored in the present work. Various symbols mark the different outcomes experienced by the various computed models, depending on initial white dwarf mass and accretion rate (see the text for symbol meanings). The results of accretion experiments performed by Livio et al. (1989) with a 1 $M_\odot$ WD are also shown at the right in the figure.

From Figure 10 it is evident that, for a constant hydrogen-accretion rate, the larger the initial mass of the white dwarf, the smaller is the mass of the helium layer required to produce a helium shell flash. Therefore, the larger the CO core mass, the smaller is the total power of the helium shell flash, even if the peak luminosity is larger. For example, during the helium shell flash in models of mass $M_{\rm WD,0} = 0.516\ M_\odot$ and $M_{\rm WD,0} = 0.8\ M_\odot$ accreting at the rate $\dot{M} \sim 10^{-7}\ M_\odot\ {\rm yr}^{-1}$, the total energy output of the model of smaller mass is larger ($\sim 0.3 \times 10^{42}$ ergs) than that of the model of larger mass ($\sim 0.5 \times 10^{41}$ ergs). Nevertheless, because of the smaller mass of the helium layer, the specific energy $E_{\rm sp}$ deposited in the envelope at the peak of the helium flash is larger in the model of larger mass: $E_{\rm sp} \sim 0.5 \times 10^{10}$ ergs g^{-1} in the model of smaller mass and $E_{\rm sp} \sim 7.1 \times 10^{10}$ ergs g^{-1} in the model of larger mass.

One of the original goals of this work was to examine the paths that a hydrogen-accreting CO white dwarf might follow to become a supernova that either ignites carbon at the center of a degenerate CO core or ignites helium in a degenerate helium layer above a CO core. The results of Livio et al. (1989) for accretion onto a white dwarf of initial mass $M_{\rm WD,0} = 1\ M_\odot$ are placed in Figure 10 to enlarge the model base. CO white dwarfs with initial masses much larger than $\sim 1.1\ M_\odot$ are not expected to form (e.g., García-Berro, Ritossa, & Iben 1997, but see Domínguez et al. 1996 for a possible way out), so the extrapolation beyond the model base that is required to cover the entire relevant domain is not extreme.

We start our analysis in the upper part of Figure 10. For accretion rates larger than $1\text{–}3 \times 10^{-7}\ M_\odot\ {\rm yr}^{-1}$ (above the line labeled "RG configuration"), the accreting star almost immediately becomes a red giant star whose external layers interact frictionally with the donor star to produce a common envelope configuration. The effect of this interaction is probably the ejection from the system of much, if not most of the matter lost by the companion (e.g., MacDonald 1980, 1986; Livio et al. 1990; Shankar, Livio, & Truran 1991). Wind mass loss also plays a role (e.g., Kato & Hachisu 1994, see also Iben & Tutukov 1996). Since hydrogen shell burning takes place at the base of the expanding envelope, if the hydrogen-rich envelope is not fully ejected, a compact helium layer is built up above the CO core. If the layer becomes massive enough, a helium shell flash takes place with the consequence that the helium layer expands to giant dimensions, leading to the loss of all hydrogen-rich matter and probably most of the helium layer. In summary, SNe Ia are not consequences of the accretion of hydrogen-rich matter at rates above the line labeled "RG configuration" in Figure 10.

A second region that is probably also excluded is the one that lies below the line labeled "Strong H pulses" in Figure 10 ($\dot{M} \sim 1\text{–}10 \times 10^{-9}\ M_\odot\ {\rm yr}^{-1}$, depending on the mass of the white dwarf). Hydrogen shell flashes produce the classical nova event in which matter is observed to be ejected from the system (by a combination of dynamical acceleration, wind mass loss, and common envelope action). In about two-thirds of observed events for which spectroscopic abundance determinations have been made, huge overabundances of elements heavier than helium are found in the ejecta, thus demonstrating that the mass of the underlying white dwarf is decreasing secularly with time. In the

other third of observed events with abundance estimates, overabundances of helium are found in the ejecta, and it is possible that, in these novae, a growing helium layer prevents the mixing with CO white dwarf matter that produces overabundances of elements heavier than helium (see the discussion in Iben & Tutukov 1996). Since all white dwarfs with CO cores born in close binary systems are expected to initially have a relatively substantial helium layer above the CO core, it may be that the further growth of this helium layer, terminated by a powerful helium shell flash that ejects the helium layer, precedes a second phase of nova outbursts that leads to a secular decrease in the mass of the CO white dwarf core.

We next address the regime of intermediate mass-accretion rates, i.e., those in the strip defined by the two lines in Figure 10 labeled "RG configuration" and "Strong H pulses" beginning with initial white dwarfs of mass 0.5–0.65 $M_\odot$. The model with the smallest accretion rate for which we have computed long-term evolution produces a very strong helium shell flash that, however, does not evolve into a detonation. Lowering the accretion rate, one enters a parameter space where recurrent shell hydrogen-burning pulses begin immediately, making a study of long-term evolutionary behavior unattractive because of the computer time required. Actually, lower accretion rates lead to longer interpulse periods, but hydrogen flashes are stronger and more time-consuming to calculate. At present, we can only guess the destiny of low-mass models accreting hydrogen-rich matter at rates smaller than some critical value (say, $\dot{M} \sim 3 \times 10^{-8}\ M_\odot\ \mathrm{yr}^{-1}$). Decreasing the accretion rate decreases the rate at which the helium layer grows in mass and increases the mean density in this layer at the beginning of a helium shell flash, an effect that acts in the direction of promoting a more explosive outcome. On the other hand, the helium layer is heated to higher temperatures by more powerful hydrogen shell flashes, an effect that acts in the opposite direction. Thus, it is not clear whether explosive helium ignition will occur, leading to a "super nova" with the dynamical ejection of the helium layer, or if the burning evolves into a quiescent regime during which the helium layer expands more gradually to giant dimensions. To remove the uncertainty, not only must the appropriate quasi-static hydrogen-accretion calculations be done, but hydrodynamical calculations with appropriate initial conditions must also be done (e.g., Tutukov & Khokhlov 1992; Woosley & Weaver 1994; Livne & Arnett 1995; Livne 1997). In any case, there is no question but that the evolution of a white dwarf accreting hydrogen-rich matter at intermediate rates is interrupted before the white dwarf attains the Chandrasekhar mass, preventing the formation of a SN Ia due to ignition of carbon at the center.

For higher accretion rates, still inside the strip and for the selected range of masses, a nondynamical off-center helium flash occurs, with a diffusion of hydrogen into the helium-burning convective zone and the formation of a detached convective shell burning hydrogen at its base. In a realistic situation, the hydrogen- and helium-rich envelope expands beyond the Roche lobe and most of the envelope is lost from the system.

Models lying in the 0.7–0.9 $M_\odot$ part of the strip, if accreting at rates smaller than $\sim 2 \times 10^{-8}\ M_\odot\ \mathrm{yr}^{-1}$, may produce dynamical ejection of the helium envelope. We cannot be sure about this possibility because it is prohibitive to follow the extremely large number of mild hydrogen-burning pulses that are required to accrete a helium layer massive enough to undergo a helium shell flash. On the other hand, models that experience a nondynamical helium shell flash when accretion rates are larger than $\sim 10^{-7}\ M_\odot\ \mathrm{yr}^{-1}$ (and probably also for rates larger than $\sim 4 \times 10^{-8}\ M_\odot\ \mathrm{yr}^{-1}$) are subject to a huge expansion of the layers surrounding the helium-burning shell. The expanded configuration is maintained also after the quenching of the helium flash, i.e., after $L_{\mathrm{He}}/L_{\mathrm{tot}}$ becomes of the order of unity. This follows also from the well-known fact that helium stars more massive than $\sim 0.8\ M_\odot$ evolve toward the red once helium is exhausted at the center, and the helium-burning shell reaches a mass larger than ~ 0.56–$0.61\ M_\odot$ (e.g., Weiss 1987; Limongi & Tornambè 1991; Fujimoto & Iben 1991; Cassisi et al. 1998). The consequence is that, in a binary system, the interaction between the expanding layers of the accreting star and the donor star forces the expulsion of most of the helium layer. An increase of the CO core mass toward the Chandrasekhar mass is therefore prevented. The same restriction holds also for accreting white dwarfs of initial mass $\sim 1\ M_\odot$.

Recently, Hachisu, Kato, & Nomoto (1996) have suggested that the Whelan & Iben (1973) model for SNe Ia—a white dwarf accreting from a Roche-lobe filling red giant—may work even if the mass ratio of donor-to-accretor exceeds what is normally considered to be the maximum for stable mass transfer. The key to their proposed solution is a balance between the tendency of a wind supported by the white dwarf to increase the orbital separation and the tendency of mass transfer to decrease orbital separation. They argue that white dwarfs initially more massive than $\sim 1\ M_\odot$ can achieve the Chandrasekhar mass and explode as SNe. Their argument requires that most of the helium layer that is built up above the CO core prior to a helium shell flash is not lost during the flash, and they support this argument by examining the effects of a wind during such a flash (Kato, Saio, & Hachisu 1989). They do not take into account the fact that the helium shell expands and that interaction with the red giant donor removes most of the expanding envelope. Further, they ascribe the strength of the white dwarf wind that they require to obtain their result to differences existing at $\log T \sim 5.2$ between OPAL opacities (Iglesias, Rogers, & Wilson 1987; Iglesias & Rogers 1991, 1993; Rogers & Iglesias 1992) and "old" Los Alamos opacity tables (Cox & Stewart 1970a, 1970b; Cox & Tabor 1976). We note that the Los Alamos opacities adopted here (Huebner et al. 1977) are very similar to the OPAL opacities, and so the expansion of the helium layer during a helium shell flash that we find cannot be ignored.

5. CONCLUSIONS

In summary, it is very difficult to see how the mass of a CO white dwarf can be increased to the Chandrasekhar mass by the accretion of hydrogen at any realistic rate. Accretion at rates in the range 1–$4 \times 10^{-8}\ M_\odot\ \mathrm{yr}^{-1}$ for a time long enough to build up a helium layer of substantial mass (~ 0.1–$0.2\ M_\odot$) leads to a helium shell flash that is probably of "super nova" proportions and dynamically ejects the helium layer.

It is a pleasure to thank L. Pacinelli for helping us prepare the figures. Partial support by the US NSF grant AST 94-17156 is acknowledged.

REFERENCES

Bragaglia, A., Greggio, L., Renzini, A., & D'Odorico, S. 1990, ApJ, 365, L13
Cassisi, S., et al. 1998, in preparation
Castellani, M., Limongi, M., & Tornambè, A. 1992, ApJ, 389, 227
Caughlan, G. R., & Fowler, W. A. 1988, At. Data Nucl. Data Tables, 40, 283
Caughlan, G. R., Fowler, W. A., Harris, M. J., & Zimmerman, B. A. 1985, At. Data Nucl. Data Tables, 32, 197
Chieffi, A., Limongi, M., & Straniero, O. 1998, ApJ, in press
Chieffi, A., & Straniero, O. 1989, ApJS, 71, 47
Cox, A. N., & Stewart, J. 1970a, ApJS, 19, 243
———. 1970b, ApJS, 19, 261
Cox, A. N., & Tabor, J. E. 1976, ApJS, 31, 271
Domínguez, I., Straniero, O., Tornambè, A., & Isern, J. 1996, ApJ, 472, 783
Fujimoto, M. Y., & Iben, I., Jr. 1991, ApJ, 374, 631
García-Berro, E., Ritossa, C., & Iben, I., Jr. 1997, ApJ, 485, 765
Giannone, P., & Weigert, A. 1967, Z. Astrophys., 67, 41
Hachisu, I., Kato, M., & Nomoto, K. 1996, ApJ, 470, L97
Hollowell, D., Iben, I., Jr., & Fujimoto, M. Y. 1990, ApJ, 351, 245
Huebner, W. F., Merts, A. L., Magee, N. H., Jr., & Argo, M. F. 1977, Los Alamos Sci. Lab. Rep. LA-6760-M
Iben, I., Jr. 1982, ApJ, 259, 244
———. 1988, ApJ, 324, 355
Iben, I., Jr., & MacDonald, J. 1995, in White Dwarfs, ed. D. Koester & K. Werner (Berlin: Springer), 45
Iben, I., Jr., & Tutukov, A. V. 1984, ApJS, 54, 335
———. 1991, ApJ, 370, 615
———. 1996, ApJS, 105, 145
Iben, I., Jr., Tutukov, A. V., & Yungelson, L. R. 1997, ApJ, 475, 291
Iglesias, C. A., & Rogers, F. 1991, ApJ, 371, L73
———. 1993, ApJ, 412, 752
Iglesias, C. A., Rogers, F., & Wilson, B. G. 1987, ApJ, 322, L45
José, J., Hernanz, M., & Isern, J. 1993, A&A, 269, 291
Kato, M., & Hachisu, I. 1994, ApJ, 437, 802
Kato, M., Saio, H., & Hachisu, I. 1989, ApJ, 340, 509
Limongi, M., Chieffi, A., Straniero, O., & Tornambè, A. 1994, Mem. Soc. Astron. Italiana, 65, 871
Limongi, M., & Tornambè, A. 1991, ApJ, 371, 317
Livio, M., Prialnik, D., & Regev, O. 1989, ApJ, 341, 299
Livio, M., Shankar, A., Burkert, A., & Truran, J. W. 1990, ApJ, 356, 250
Livne, E. 1997, in Thermonuclear Supernovae, ed. P. Ruiz-Lapuente, R. Canal, & J. Isern (Dordrecht: Kluwer), 425
Livne, E., & Arnett, D. 1995, ApJ, 452, 62
MacDonald, J. 1980, MNRAS, 191, 193
———. 1986, ApJ, 305, 251
Marsh, T. R. 1995, MNRAS, 275, L1
Marsh, T. R., Dhillon, V. S., & Duck, S. R. 1995, MNRAS, 275, 828
Mochkovich, R., & Livio, M. 1990, A&A, 236, 378
Nomoto, K., Nariai, K., & Sugimoto, D. 1979, PASJ, 31, 287
Nomoto, K., & Sugimoto, D. 1977, PASJ, 29, 765
Paczyński, B., & Żytkow, A. N. 1978, ApJ, 222, 604
Robinson, E. L., & Shafter, A. W. 1987, ApJ, 332, 296
Rogers, F., & Iglesias, C. A. 1992, ApJS, 79, 507
Ross, J. E., & Aller, L. H. 1976, Science, 191, 1223
Shankar, A., Livio, M., & Truran, J. W. 1991, ApJ, 374, 693
Sion, E. M., Acierno, M. J., & Tomczyk, S. 1979, ApJ, 230, 832
Sion, E. M., & Starrfield, S. 1986, ApJ, 303, 130
Starrfield, S., Sparks, W. M., & Truran, J. W. 1974a, ApJS, 28, 247
———. 1974b, ApJ, 192, 647
Tutukov, A. V., & Khokhlov, A. M. 1992, Soviet Astron., 36, 401
van den Heuvel, E. P. J., Bhatacharya, D., Nomoto, K., & Rappaport, S. A. 1992, A&A, 262, 97
Webbink, R. F. 1984, ApJ, 277, 355
Weiss, A. 1987, A&A, 185, 165
Whelan, J. C., & Iben, I., Jr. 1973, ApJ, 186, 1007
Woosley, S. E., & Weaver, T. A. 1994, ApJ, 423, 371